

Lightning Activity in the Southern Coast of Chile

M. Gabriela Nicora^{1,*}, René D. Garreaud², Rodrigo E. Bürgesser³, Eldo E. Ávila³, Eduardo J. Quel¹

1. CEILAP, UNIDEF (MINDEF-CONICET), Villa Martelli, Buenos Aires, Argentina,

2. Department of Geophysics, Universidad de Chile and Center for Climate and Resilience Research,
Santiago, Chile

3. FaMAF, Universidad Nacional de Córdoba, IFEG-CONICET, Córdoba, Argentina

ABSTRACT: Based on eight years of lightning data (from January 2005 to December 2012) from the World Wide Lightning Location Network (WWLLN) we describe the spatial distribution and temporal variability of lightning activity over southern Chile. This region extends from $\sim 40^{\circ}\text{S}$ to 55°S along the west coast of South America, is limited to the east by the austral Andes about 100 km inland, and features a maritime climate with annual mean precipitation in excess of 4000 mm.

Cloud electrification is not expected in this region given the predominance of stable, deep-stratiform precipitation there, but days with at least one stroke occur up to a third of the time along the coast, being slightly more frequent during late summer and fall.

Lightning density and frequency of lightning days exhibit a sharp maximum along the coast of southern Chile. Disperse strokes are also observed off southern Chile. In contrast, lightning activity is virtually inexistent over the austral Andes -where precipitation is maximum- and farther east over the dry lowlands of Argentina.

It is suggested that electrification could develop under weakly unstable conditions that prevail in the region after the passage of a cold front. Large-scale ascent near the cyclone's center may lift near-surface air parcels over open ocean fostering shallow convection, which is enhanced as the strong westerly flow ascend over the coastal topography. Laboratory experiments of charge transferred during ice crystal-graupel collisions in low liquid water content conditions and low impact velocity have shown that the non-inductive mechanism can work as a charge separation process in these systems.

.

INTRODUCTION

Frontal cyclones drifting eastward along the oceanic storm tracks are responsible for most of the precipitation and day-to-day weather variations in the extratropics. These storms are dominated by clouds and precipitation of stratiform nature [e.g., Houze 1993, chapter 9]. Consistently, they exhibit modest lightning activity relative to deep convective systems over warm land masses. Indeed, global lightning climatologies constructed on the basis of satellite data [e.g., Christian et al. 2003] and ground-based networks [Virts et al. 2013] reveal that the mean lightning density over the oceans poleward of 40° is 50 to 500 times smaller than the lightning density over tropical/subtropical land masses.

Lightning activity is markedly low (sparse satellite coverage and fewer ground-based receivers to the

* San Juan Bautista de La Salle 4397 (B1603ALO), Villa Martelli (Buenos Aires - Argentina), gabriela@blueplanet.com.ar

south of 40°S may exacerbate this condition) along the Southern Hemisphere storm track, that is collocated with the westerly wind belt between 45°–55°S [e.g., Hoskins and Hodges 2005]. Annual mean rainfall across much of the Southern Oceans is about 1000-1500 mm but this value changes dramatically as the storm track intercepts Patagonia in the southern tip of South America [e.g., Garreaud et al. 2013]. This region extends southward from about 40°S and is divided by the austral Andes (i.e., the southern extent of this mountain range); sea surface temperatures (SST) over the adjacent Pacific Ocean don't surpass 10°C. Orographic enhancement upstream of the mountains results in copious precipitation over Western Patagonia (Chilean side). The actual precipitation distribution is poorly constrained, because of the minimum rain gauge network in this extremely inaccessible region, but the annual mean accumulation ranges between 5.000 and 10.000 mm/year supporting extensive rainforests, major rivers and the Northern and Southern Patagonia ice fields. Mean precipitation decreases to less than 300 mm/yr just a few tens of kilometers downstream of the continental divide, leading to one of the most dramatic precipitation gradients on Earth [Smith and Evans 2007].

Based on the previous background, conventional wisdom suggests little –if any– lightning activity over the cool, hyper-humid Western Patagonia. Two lines of evidence, however, suggest that lightning in that region does occur rather frequently. First, paleo-environmental reconstructions based on tree samples and lake sediments have documented significant, wildfire activity over Western Patagonia during the Holocene [Holz and Veblen 2011ab]. Secondly, the World Wide Lightning Location Network (WWLLN), a ground-based network, allows a global, real-time monitoring of lightning activity for ~1700 volcanoes to detect ash cloud lightning signaling an ongoing volcanic eruption (<http://wwlln.net/volcanoMonitor.html>). The southern Andes hosts more than 33 active volcanoes but their eruption is rare (e.g., three major events in the last decade, Sernageomin 2012). In contrast, we noted WWLLN volcanic warnings 4-5 times per month over southern South America, that were subsequently interpreted as weather-related events.

In this work we precisely study lightning activity over Western Patagonia. Our study relies on 8-year data from the WWLLN along with other sources of meteorological information.

DATA

In this work we have used WWLLN data from January 2005 to December 2012, with emphasis on the occurrence of lightning over the Western Patagonia and the adjacent Pacific to the south of ~40°S. The WWLLN detection efficiency (DE) in this region is unknown and it changed over time (there is no in-situ lightning detection network and the data from the Lightning Imaging Sensor on board of the TRMM satellite is limited to ~38° of latitude) but it is likely between 5-10%, the global efficiency estimated elsewhere [Rudlosky and Shea 2013]. We have also used historical records of thunderstorm days on a handful of stations in Patagonia compiled by the World Meteorological Organization [WMO, 1953].

The atmospheric circulation and thermodynamic conditions during lightning-producing storms were characterized using the Climate Forecast System Reanalysis (CFSR) elaborated by the National Centers for Environmental Prediction (NCEP). The high-resolution of CFSR is particularly useful when examining specific storms over Western Patagonia, in conjunction with WWLLN data and visible (channel 1) and thermal infrared (channel 4) satellite images from GOES 13 archived in the NOAA Comprehensive Large Array-data Stewardship System (CLASS; <http://www.class.ncdc.noaa.gov/>).

To provide context to our lightning climatology we describe the annual mean precipitation field

obtained from several sources. Over land we used the long-term (at least 30 years of data) average values from rain gauges operated by the Chilean weather service and water authority and offshore, we used the long-term-mean values from the NOAA NCEP Climate Prediction Center Merged Analysis of Precipitation [CMAP, Xie and Arkin 1996].

SPATIAL AND TEMPORAL DISTRIBUTION

Let us begin our analysis by displaying the lightning density (ρL) and the number of days with lightning (N_d) (Fig. 1a,b). The lightning density is defined here as the count of strokes in non-overlapping $0.1^\circ \times 0.1^\circ$ lat-lon grid boxes considering the whole record (Jan. 2005 - Dec. 2012) divided by 8 years, so it has units of strokes per ~ 100 km² per year. The number of days with lightning is the count of days with a least one stroke in $0.25^\circ \times 0.25^\circ$ lat-lon grid boxes considering the whole record divided by 8 years, so it has units of days per year. The grid box sizes are somewhat arbitrary and don't necessarily coincide with other work's definitions, but they allow us to detect the detailed structure of ρL and N_d as well as regional differences.

The ρL and N_d maps have a similar, well defined structure, with a sharp maximum along the Chilean coast from 42° to $52^\circ S$. This coastal band of maximum in ρL and N_d is collocated with the maximum in precipitation and number of rainy days derived from high-resolution, satellite based products (the SSM/I rain-rate estimates; Fig. 2 in Falvey and Garreaud 2007) and a local maximum in CFSR convective rainfall rate (not shown). Lightning activity is virtually nonexistent over the austral Andes, including the massive Northern and Southern Patagonia Ice fields. Very low lightning activity is found over the dry lowlands to the east of the austral Andes, but ρL and N_d increase equatorward reaching values comparable to those in Western Patagonia to the north of $38^\circ S$

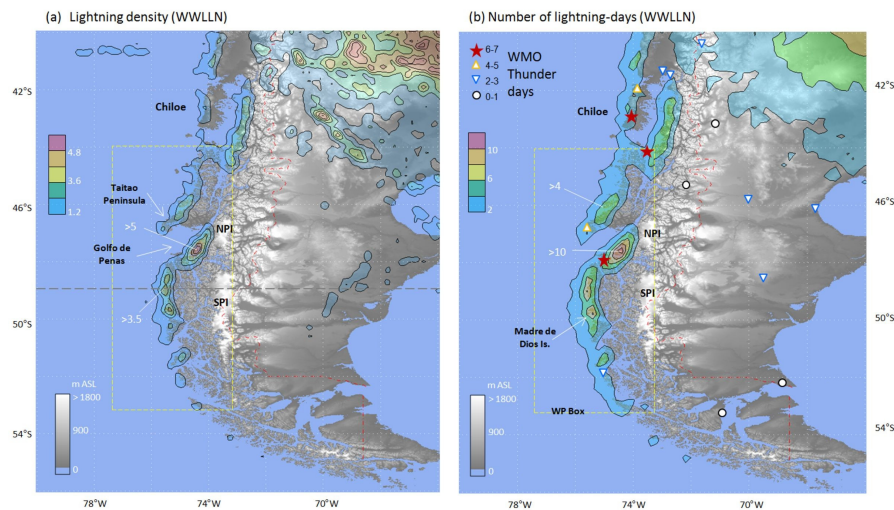


Figure 1. (a) Lightning density contoured every 1.2 stroke in $0.1^\circ \times 0.1^\circ$ lat-lon grid boxes per year. (b) Number of lightning days (at least one stroke in $0.25^\circ \times 0.25^\circ$ lat-lon grid boxes per year) contoured every 2 days per year.. Symbols in panel (b) are the annual mean number of thunderstorm days from WMO [1953].

The temporal behavior of the lighting activity in southern Chile is illustrated by the time series of the daily number of strokes in Western Patagonia box (42-54°S / 76-70°W, see Fig. 1) for year 2012 (Fig. 2a). Because the strokes are highly clustered on a few spots along the coast, our results are not sensitive to the box definition. During 2012 there were 125 lightning days; other years show a similar behavior (not shown) and the yearly number of lightning days in the Western Patagonia box varies from 107 in 2008 to 151 in 2012. The total number of strokes in this box ranged from 1665 in 2010 to 5689 in 2012, with a mean value of 3013 and a standard deviation of 1335, possible as a consequence of changes in DE and natural variability. Lightning activity concentrates in events of 1-4 day duration recurring a few times per month; most of these days have less than 10 strokes in the Western Patagonia box but in 10% of them the number of strokes exceeds 50. Figure 2a also includes CFSR total precipitation over the Western Patagonia box which is highly recurrent there (nearly 70% of the time); lightning days are accompanied by precipitation all the time but there are many precipitation days with no lightning.

Using the 8-year record, the monthly average number of lightning days (as well as days with more than 10 strokes) in the Western Patagonia box is shown in Fig. 2b. Consistent with a small thermal forcing at high latitudes, the lightning activity in Western Patagonia exhibits a weak annual cycle. Lightning activity, however, tends to be more frequent from summer in the SH (DJF) to late fall, peaking in March-April, and somewhat lower in late winter and spring (see also Fig. 2a). Likewise, the number of station-based thunderstorm days in Western Patagonia is slightly larger in summer and fall [WMO 1953]. We also verified that the lightning density pattern in every month and season is very similar to the annual map (Fig. 1), with a sharp maximum in lightning activity along the Western Patagonia coast where strokes occur in nearly a third of days.

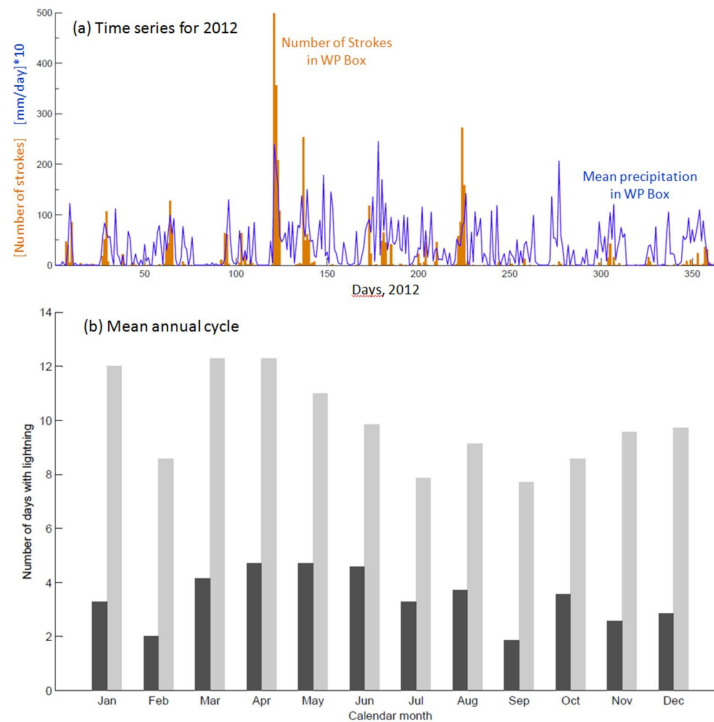


Figure 2. (a) Time series of the number of WWLLN strokes and CFSR total precipitation in the Western

Patagonia Box (42-54°S / 76-70°W, see Fig. 3) during year 2012. (b) Black bars: monthly mean (over the 8-year record) number of days with at least 1 strokes over Western Patagonia box; gray bars: as before but for the monthly mean number of days with at least 10 strokes. Data from WLLN, Jan. 2005 - Dec. 2012

CLIMATOLOGICAL ANALYSIS

A cursory inspection of the weather maps and satellite imagery for several cases of significant lightning activity in Western Patagonia reveals a similar synoptic environment. These conditions are synthesized here using a compositing analysis of selected meteorological fields for the 90 days on record with more than 50 strokes in the Western Patagonia Box. The lightning distribution for this sub-sample of days follows the full-sample spatial pattern (not shown).

The composite maps of sea level pressure (SLP) and 925 hPa air temperature (Fig. 3a) show a low pressure center west of the Drake Passage and the incursion of cold air over the southeast Pacific extending along the Chilean coast up to ~40°S. The location of the composite low pressure area (very close to the cyclone position in the case study) reflects that nearly all the lightning-producing storms in Western Patagonia were associated with a deep low over the southeast Pacific (also note the cyclone's central position for selected cases). Likewise, a cold front making landfall *to the north* of Western Patagonia was a highly common feature of these storms, evidenced in our composite analysis by a baroclinic zone in the low-level air temperature (Fig. 3a) and a tongue of moist air ahead of the front in the map of precipitable water anomalies (Fig. 3d). Thus, significant lightning activity in Western Patagonia most often occurs as the postfrontal air mass has reached this region. Figure 11b shows the composite anomalies of SLP and the 300 hPa geopotential height. Negative anomalies are collocated just to west of the tip of the continent, indicative of the barotropic structure, mature stage of the midlatitude cyclone that drifted slowly eastward.

Negative temperature anomalies in the middle and lower troposphere (Fig. 3c) are also located off Western Patagonia. Along the coast of southern Chile the composite 500-hPa cooling is much larger (~4°C) than the cooling at low levels (<1°C), leading to the development of a broad area of convective instability in the postfrontal air mass that encompasses Patagonia and the adjacent Pacific. To illustrate such unstable conditions Fig. 3d shows the composite map of the surface lifted index (LI) with near-zero values over Western Patagonia and offshore. We choose the lifted index given its normal distribution, more suitable for the compositing analysis, but other stability indices show a similar pattern (e.g., CAPE; not shown). It is within this weakly unstable region where most lightning occur.

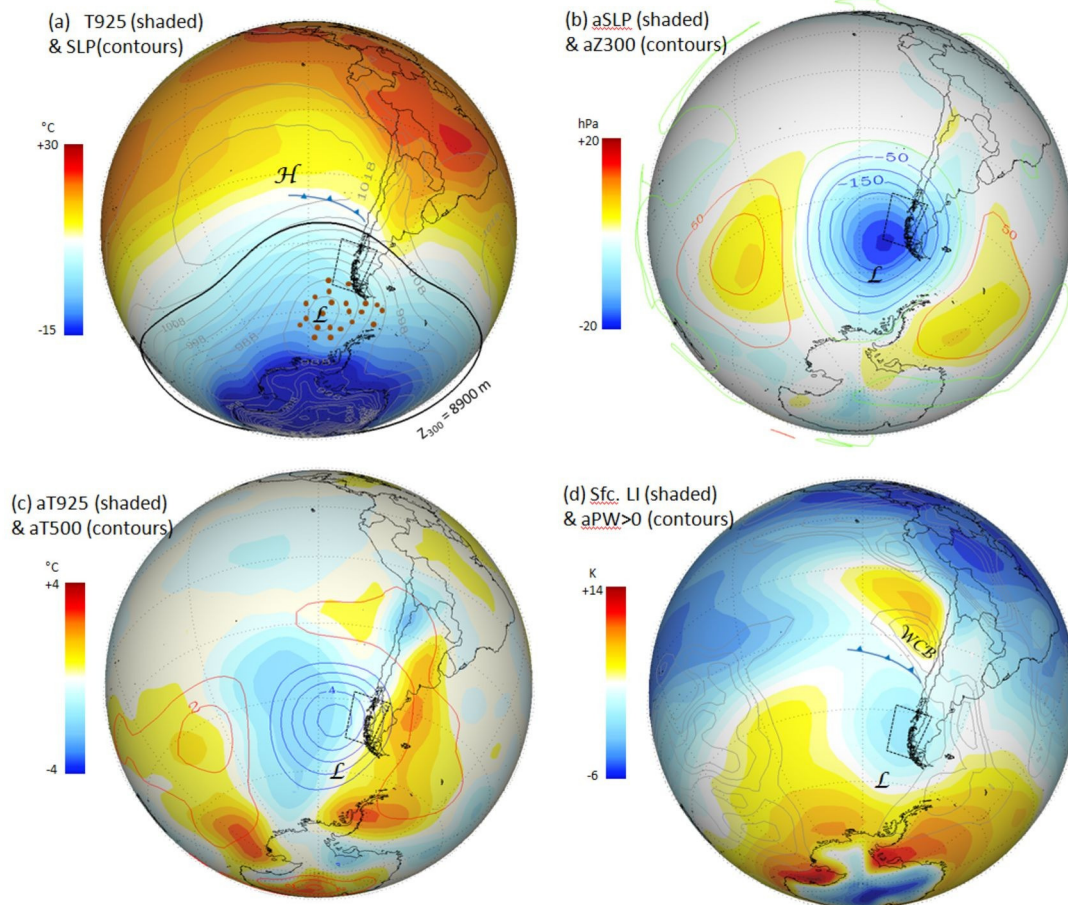


Figure 3. Composite maps of selected CFSR meteorological fields for the 90 days with more than 50 strokes in the Western Patagonia box (dashed box). (a) Sea level pressure (SLP) contoured every 5 hPa and 925 hPa air temperature (shaded, scale at left). Also indicated is the cyclone's core for selected cases (red dots) and the most common location of the cold front over the southeast Pacific. (b) SLP anomalies (shaded, scale at left) and 300 hPa geopotential height anomalies (contoured every 50 mgp). Anomalies are calculated as departure from the long-term-mean. (c) 925-hPa air temperature anomalies (shaded, scale at left) and 500 hPa air temperature anomalies (contoured every 1 °C). (d) Surface lifted index (shaded, scale at left) and precipitable water anomaly (contoured at 5, 10, 15 and ≥ 20 cm). The letter L indicates the average cyclone center and WCB is the mean location of the warm conveyor belt. Vertical perspective (globe view from finite distance)

CONCEPTUAL MODEL AND CONCLUDING REMARKS

Eight years of global stroke detection from the WLLN has allowed to identify a maximum of lightning activity over Western Patagonia (42°-52°S), a cool, hyper-humid region located just downstream of the South Pacific storm track and bounded to the east by the Austral Andes. Cloud electrification is not expected in this region given the predominance of stable, deep-stratiform precipitation there, but days with at least one stroke occur up to a third of the time along the coast, being slightly more frequent during late summer and fall.

Lightning-producing storms last 1-3 days and develop under a recurrent synoptic environment

identified in a case study and generalized by a compositing analysis of 90 events. A key ingredient is a deep surface cyclone over the South Pacific – Drake Passage, often below a closed upper-level low pressure, indicative of the mature stage of the disturbance. By the day of significant lightning activity the attending cold front has reached the coast of southern Chile at about 40°S so that Western Patagonia is immersed in the postfrontal sector of the system. During these sub-Antarctic air incursions, the cooling above 700 hPa occurs before and is more pronounced than the cooling at lower levels, leading to a weakly unstable environment off the coast of southern Chile (CAPE~100 J/Kg; LI ~ 0°C). Most of the strokes are located right along the coast and some strokes occur offshore where shallow, open cell clouds are readily identifiable and convective rainfall dominates. In contrast, few (or no) strokes are observed along the cold front or the austral Andes where the precipitation maximizes.

We interpret this conspicuous spatial structure as follows. Under the weakly unstable conditions that prevail in the postfrontal air mass, large-scale ascent near the cyclone's center may lift near-surface air parcels over open ocean fostering shallow convection and disperse lightning activity. Near the coast a second ingredient comes into play. The moderate to strong westerly flow impinges over the coastal mountains that rise sharply to 300-700 m ASL, forcing a rapid uplift of the marine air that trigger convection and produces significant lightning activity. Forced ascent continues farther inland but the cold, ice-covered surface precludes the development of convection. Clearly, *in-situ* measurements (e.g., coastal radiosondes) are much necessary to validate this conceptual model. Furthermore, the numerical values of lightning density in this region are dependent on the WWLLN detection efficiency, which is variable and unknown over this region due to lack of independent measurements. By the contrary, the spatial pattern of the lightning density as well as the number of days with lightning appears more robust.

In addition to the prominent coastal topography, the confinement of significant lightning activity off Western Patagonia seems also associated with the surface boundary conditions over the adjacent Pacific. Although cold SST (<10°C) prevails year round, these offshore waters are up to 3°C warmer than those over open ocean producing the most favorable conditions for instability build up than anywhere else in the southeast Pacific when a mid-level cold anomaly passes over (Fig. 4).

The relatively warm coastal waters are due to the coastal downwelling and poleward flow generated by the West Wind Drift. Therefore, seasonal, interannual and longer-time fluctuations in the intensity and position of this current may modulate changes in the lightning activity in Western Patagonia.

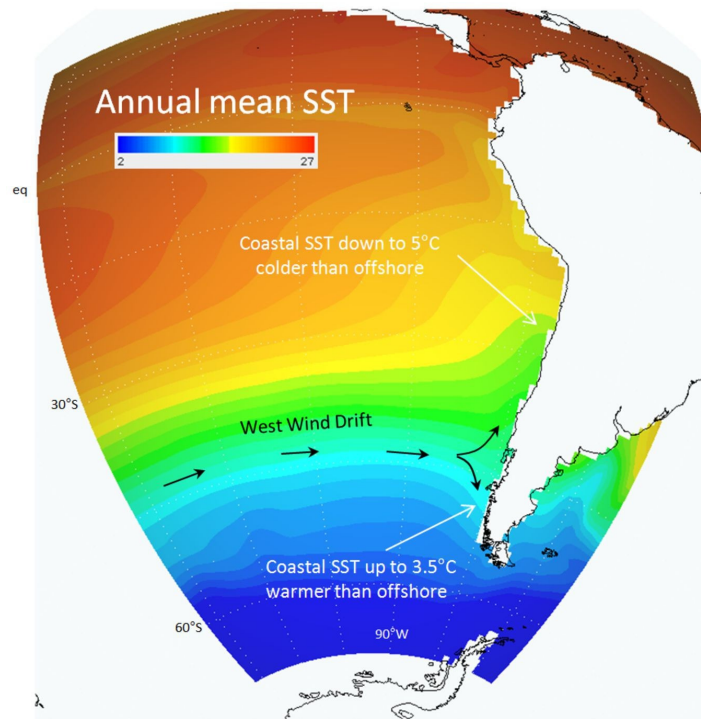


Figure 14. NCEP optimally interpolated annual mean Sea Surface Temperature over the eastern Pacific. Note how the zonal symmetry over Open Ocean breaks down along the Chilean coast, specially off Western Patagonia. Vertical perspective (globe view from finite distance).

ACKNOWLEDGMENTS

The authors wish to thank the World Wide Lightning Location Network (<http://wwlln.net>), collaboration among over 60 universities and institutions, for providing the lightning location data used in this paper. The manuscript was improved considerably through the comments and suggestions by three anonymous reviewers. RG was supported by FONDECYT-Chile (Grant 1110169) and FONDAP/CONICYT Chile (Grant 15110009 - CR2). This work was supported by SECYT-UNC, CONICET and FONCYT, and PIDDEF 14/12, MINDEF Argentina

REFERENCES

- Christian, H. J., R. J. Blakeslee, D. J. Boccippio, W. L. Boeck, D. E. Buechler, K. T. Driscoll, S. J. Goodman, J. M. Hall, W. J. Koshak, and D. M. Mach (2003), Global frequency and distribution of lightning as observed from space by the Optical Transient Detector. *J. Geophys. Res.*, 108, 4005, doi:10.1029/2002JD002347
- Falvey, M. and R. Garreaud (2007), Wintertime precipitation episodes in central Chile: Associated meteorological conditions and orographic influences. *Journal of Hydrometeorology*, 8, 171-193.

- Garreaud, R., P. Lopez, M. Minvielle, and M. Rojas (2013), Large-Scale Control on the Patagonian Climate, *Journal of Climate*, 26, 215-230.
- Holz, A. and T. T. Veblen (2011a), The amplifying effects of humans on fire regimes in temperate rainforests in Western Patagonia, *Palaeogeography, Palaeoclimatology, Palaeoecology*, 311, 82-92.
- Holz, A. and T. T. Veblen (2011b), Variability in the Southern Annular Mode determines wildfire activity in Patagonia, *Geophysical Research Letters*, 38.
- Hoskins, B. J. and K. I. Hodges (2005), A new perspective on Southern Hemisphere storm tracks, *Journal of Climate*, 18, 4108-4129.
- Houze Jr, R. A., 1994: *Cloud dynamics*. Vol. 53, Elsevier, 523 pp.
- Rudlosky, S. D., and D. T. Shea (2013), Evaluating WWLLN Performance Relative to TRMM/LIS, *Geophys. Res. Lett.*, 40, 2344–2348, doi:10.1002/grl.50428
- Smith, R. and J. Evans (2007) Orographic precipitation and water vapor fractionation over the southern Andes, *Journal of Hydrometeorology*, 8, 3-19.
- Virts, K. S., J. M. Wallace, M. L. Hutchins, and R. H. Holzworth (2013), Highlights of a new ground-based, hourly global lightning climatology. *Bulletin of the American Meteorological Society*. 94, 1381–1391. doi: <http://dx.doi.org/10.1175/BAMS-D-12-00082.1>
- World Meteorological Organization [WMO] (1953), *World distribution of thunderstorm days. Part I: Tables*. Geneva, 213 pp.
- Xie, P. and P. A. Arkin (1997), Global precipitation: A 17-year monthly analysis based on gauge observations, satellite estimates, and numerical model outputs, *Bulletin of the American Meteorological Society*, 78, 2539-2558.